

Anticyclonic suppression of the North Pacific transient eddy activity in midwinter

Satoru Okajima¹, Hisashi Nakamura², and Yohai Kaspi³

¹The University of Tokyo

²University of Tokyo

³Weizmann Institute of Science

October 17, 2023

Abstract

Dynamical understandings of midlatitude transient eddy activity, especially its midwinter minimum over the North Pacific, are still limited, partly because Eulerian eddy statistics are incapable of separating cyclonic and anticyclonic contributions. Here we evaluate the two contributions separately based on local curvature of instantaneous flow fields to compare their seasonality between the North Pacific and North Atlantic storm-tracks. The anticyclonic contribution is found crucial for the midwinter minimum of the North Pacific transient eddy activity. Eddy energetics reveals that the net efficiency of the anticyclonic contribution in replenishing total transient eddy energy over the North Pacific exhibits a pronounced midwinter minimum, while that of the cyclonic counterpart does not in harmony with precipitation that peaks around midwinter. This study suggests that more attention should be paid to anticyclones in studying midlatitude storm-track dynamics.

Hosted file

970766_0_art_file_11319457_rzvzrd.docx available at <https://authorea.com/users/601690/articles/661653-anticyclonic-suppression-of-the-north-pacific-transient-eddy-activity-in-midwinter>

Hosted file

970766_0_supp_11314811_rztjv7.docx available at <https://authorea.com/users/601690/articles/661653-anticyclonic-suppression-of-the-north-pacific-transient-eddy-activity-in-midwinter>

1
2 **Anticyclonic suppression of the North Pacific transient eddy activity in midwinter**

3
4 **Satoru Okajima¹, Hisashi Nakamura¹, Yohai Kaspi²**

5
6 ¹Research Center for Advanced Science and Technology, The University of Tokyo, Tokyo,
7 Japan

8 ²Department of Earth and Planetary Sciences, Weizmann Institute of Science, Rehovot, Israel

9
10 Corresponding author: Satoru Okajima (okajima@atmos.rcast.u-tokyo.ac.jp)

11
12
13 **Key Points:**

- 14 • Anticyclonic contribution is crucial for the midwinter minimum of the North Pacific
15 transient eddy activity
- 16 • Anticyclonic suppression is consistent with a midwinter minimum of the net efficiency of
17 energy conversion/generation terms
- 18 • More attention should be paid to anticyclones in studying midlatitude storm-track
19 dynamics
20
21

22 **Abstract**

23 Dynamical understandings of midlatitude transient eddy activity, especially its midwinter
24 minimum over the North Pacific, are still limited, partly because Eulerian eddy statistics are
25 incapable of separating cyclonic and anticyclonic contributions. Here we evaluate the two
26 contributions separately based on local curvature of instantaneous flow fields to compare their
27 seasonality between the North Pacific and North Atlantic storm-tracks. The anticyclonic
28 contribution is found crucial for the midwinter minimum of the North Pacific transient eddy
29 activity. Eddy energetics reveals that the net efficiency of the anticyclonic contribution in
30 replenishing total transient eddy energy over the North Pacific exhibits a pronounced midwinter
31 minimum, while that of the cyclonic counterpart does not in harmony with precipitation that
32 peaks around midwinter. This study suggests that more attention should be paid to anticyclones
33 in studying midlatitude storm-track dynamics.

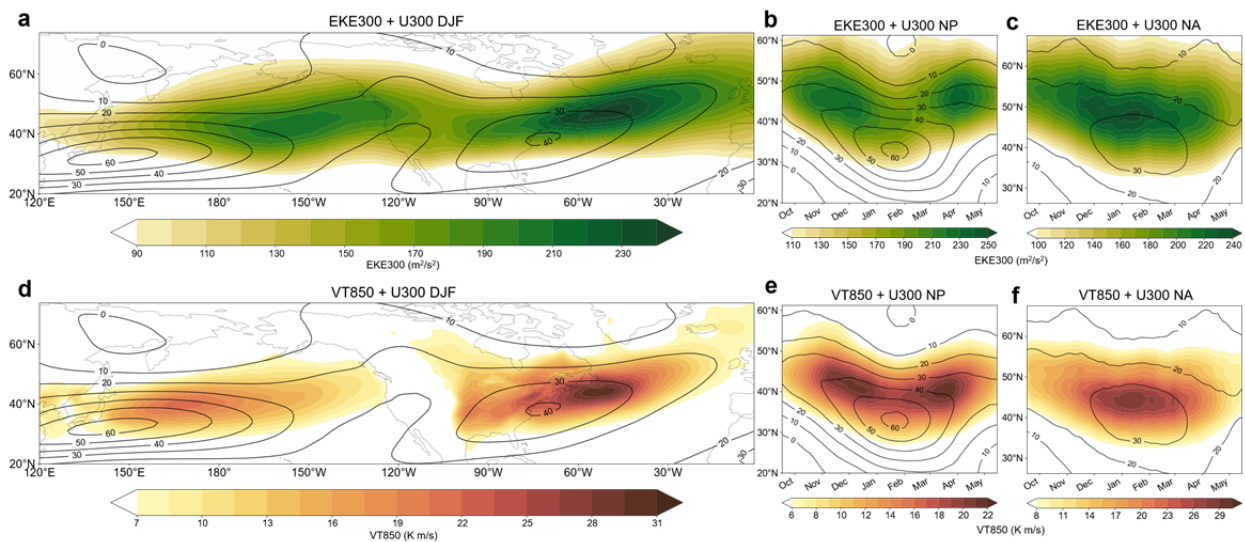
34

35 **Plain Language Summary**

36 Our understanding of the dynamics of midlatitude transient eddy activity, especially its
37 midwinter minimum over the North Pacific, is still limited. This is partly because conventional
38 local statistics based on temporal filtering, which are commonly used as a measure of transient
39 eddy activity, are unable to treat contributions from cyclones and anticyclones separately. Here
40 we evaluate cyclonic and anticyclonic contributions to local eddy statistics separately based on
41 local curvature of instantaneous flow fields, to compare their seasonality between the North
42 Pacific and North Atlantic storm-tracks. The anticyclonic contribution is found crucial for the
43 midwinter minimum of the North Pacific transient eddy activity. We further apply eddy
44 energetics to investigate the relative importance of processes relevant to the maintenance of
45 storm-tracks. The net efficiency of the relevant processes associated with the anticyclonic
46 contribution in replenishing total transient eddy energy over the North Pacific exhibits a
47 pronounced midwinter minimum. By contrast, that of the cyclonic counterpart does not in
48 harmony with precipitation that peaks around midwinter. This study suggests that more attention
49 should be paid to anticyclones in studying midlatitude storm-track dynamics.

50 **1 Introduction**

51 Midlatitude transient eddies that give rise to day-to-day weather variability are one of the
 52 rudimentary components of the Earth’s climate system (Hurrell, 1995; Shaw et al., 2016).
 53 Blackmon (1976) suggested that regions of large band-pass (with periods of 2–6 days) variance
 54 of geopotential height correspond to those of frequent cyclone passage over the North Atlantic
 55 (NA) and North Pacific (NP) basins, referring to them as “storm-tracks”. Those regions are
 56 characterized by prominent lower-tropospheric poleward eddy heat flux (Fig. 1) (Blackmon et
 57 al., 1977), indicative of baroclinic development of migratory cyclones. Those storm-tracks are
 58 collocated with the low-level eddy-driven jets and associated baroclinic zones (Nakamura et al.,
 59 2004), and maintained through the effective restoration under the influence of major oceanic
 60 frontal zones (Hotta & Nakamura, 2011; Kaspi & Schneider, 2011, 2013).



61
 62 **Figure 1. Wintertime climatological-mean transient eddy activity and its seasonality. a**
 63 Climatological-mean wintertime (DJF-mean) EKE_{300} (color, m^2/s^2). Contours denote
 64 climatological-mean westerly wind speed (U_{300} ; m/s). **b-c** Climatological seasonality in EKE_{300}
 65 averaged for $180^\circ\text{--}150^\circ\text{W}$ (c) and $60^\circ\text{--}30^\circ\text{W}$ (d). Contours denote the corresponding seasonality
 66 of U_{300} averaged for $150^\circ\text{E--}180^\circ$ (c) and $70^\circ\text{--}40^\circ\text{W}$ (d). A tick mark on the abscissa in b-c
 67 represents the first day of a given calendar month. **d-f** Same as in a-c, respectively, but for
 68 $V'T'_{850}$ (color, K m/s), averaged over $150^\circ\text{E--}180^\circ$ (e) and $70^\circ\text{--}40^\circ\text{W}$ (f).

69 Eulerian statistics are compatible with quantitative analyses and dynamical diagnostics
 70 (Eyering et al., 2021). The eddy energetics is useful for investigating the formation and
 71 maintenance mechanisms for the mean westerlies and storm-tracks (Chang et al., 2002; Okajima
 72 et al., 2022; hereafter ONK22). Based on Eulerian statistics, the climatological-mean seasonality
 73 of storm-track activity, the maintenance mechanisms for the westerly jets and storm-tracks, and
 74 their relationship with the lower-boundary condition have been well documented (Chang et al.,
 75 2002; Lee & Kim, 2003; Nakamura et al., 2004; Kaspi and Schneider, 2013).

76 Nevertheless, dynamical understandings of midlatitude transient eddy activity are still
 77 limited, especially for the “midwinter minimum (MWM)” or “midwinter suppression” of the NP
 78 transient eddy activity (Nakamura, 1992). Under the maximized upper-level jet speed, the
 79 climatological-mean NP transient eddy activity exhibits a clear minimum in midwinter as

80 measured by eddy kinetic energy at 300-hPa (EKE_{300}) (Fig. 1b) and poleward eddy heat transport
81 at 850-hPa ($V'T'_{850}$) (Fig. 1e). This MWM is inconsistent with the baroclinic instability theory
82 (Eady, 1949) and sharply contrasts with the climatological midwinter maximum of the NA
83 transient eddy activity (Figs. 1c and 1f). Various mechanisms have been proposed for this
84 phenomenon, including barotropic (James, 1987) and baroclinic (Schemm & Rivière, 2019)
85 aspects of eddies, diabatic heating (Chang, 2001), trapping of upper-level eddies into the
86 subtropical jet core (Nakamura & Sampe, 2002), an upstream influence (Penny et al., 2010), and
87 structures of the jet streams (Deng & Mak, 2005; Yuval et al., 2018). Based on the
88 comprehensive energetics of transient eddies, ONK22 suggested that multiple processes must be
89 responsible for the MWM. The dynamical origin of the MWM thus remains elusive.

90 The MWM of the NP transient eddy activity has recently been also investigated through
91 the Lagrangian approach by conducting feature tracking (Schemm & Rivière, 2019; Hadas &
92 Kaspi, 2021). Most of those studies, however, have focused only on migratory cyclones.
93 Okajima et al. (2023; hereafter ONK23) recently revealed that the climatological-mean density
94 of NP surface migratory anticyclones exhibits a clear MWM, while the cyclonic counterpart
95 peaks in midwinter. This suggests that anticyclones are likely key to understanding the
96 mechanisms for the MWM of the NP transient eddy activity. This hypothesis is compatible with
97 the midwinter peak in the climatological-mean precipitation over the NP as well as over the NA
98 (Supplementary Fig. S1), implying that cyclonic activity may not minimize in midwinter even in
99 the NP.

100 Therefore, whether anticyclones are indeed important for the MWM of the NP transient
101 eddy activity measured by Eulerian eddy statistics needs to be investigated. However, traditional
102 Eulerian eddy statistics are incapable of separating cyclonic and anticyclonic contributions
103 (Wallace et al., 1988). Recently, a novel method to identify three-dimensional regions of
104 individual cyclonic and anticyclonic rotations was proposed (Okajima et al., 2021; hereafter
105 ONK21). The method enables evaluating cyclonic and anticyclonic contributions separately in
106 Eulerian eddy statistics and atmospheric energetics, as a “hybrid” method into which both
107 Eulerian and Lagrangian perspectives are incorporated.

108 This study thus aims to investigate the seasonality of the cyclonic and anticyclonic
109 contributions to transient eddy activity and energetics within the NP and NA storm-tracks. We
110 will demonstrate that anticyclones are more important for the MWM of the NP transient eddy
111 activity, to argue that more attention should be paid to migratory anticyclones in studying
112 midlatitude storm-track dynamics.

113 **2 Data and Methods**

114 **2.1 Atmospheric reanalysis**

115 We analyze 6-hourly global fields of atmospheric variables, including geopotential
116 height, air temperature, wind velocity, and diabatic heating rates in pressure coordinates, in
117 addition to sea-level pressure, obtained from the Japanese 55-year atmospheric reanalysis (JRA-
118 55) by the Japan Meteorological Agency (JMA) (Kobayashi et al., 2015; Harada et al., 2016) for
119 the period 1958-2022. Variables at selected pressure levels are available on a $1.25^\circ \times 1.25^\circ$ grid.
120 At each grid point, fluctuations of a given variable with synoptic-scale transient eddies have been
121 extracted locally from the 6-hourly reanalysis data as its deviations from their low-pass-filtered

122 fields through a 121-point Lanczos filter with a cutoff period of 8 days. Plots showing seasonal
 123 evolutions (as in Fig. 1) are produced after applying a 31-day running mean to daily climatology.

124 2.2 Cyclonic and anticyclonic contributions to Eulerian eddy statistics

125 Climatological-mean eddy Eulerian statistics are calculated separately for cyclonic and
 126 anticyclonic contributions based on two-dimensional local flow curvature κ_2 (ONK21). It is
 127 calculated at a given vertical level instantaneously from horizontal winds as

$$128 \quad \kappa_2 \equiv \frac{1}{R_S} = \frac{1}{V^3} (-uvv_x + u^2v_x - v^2u_y + uvv_y),$$

129 where R_S denotes the curvature radius, V scalar wind speed, and a subscript denotes zonal or
 130 meridional derivative, respectively. A positive (negative) value signifies a cyclonic
 131 (anticyclonic) rotation in the Northern Hemisphere. This method effectively removes the effect
 132 of shear vorticity, associated with the strong westerlies and requires no temporal filtering to
 133 determine the shape of the regions of rotations. We use unfiltered winds to calculate curvature as
 134 in ONK23, who conducted tracking of surface migratory cyclones and anticyclones based on
 135 unfiltered SLP. It also helps to retain asymmetry between cyclonic and anticyclonic rotations
 136 (e.g., gradient wind balance).

137 Separate contributions from cyclonic and anticyclonic regions to Eulerian statistics are
 138 evaluated by accumulating instantaneous contributions only at grid points where cyclonic or
 139 anticyclonic curvature is observed (ONK21), as a practical, *ad hoc* method. In this study, the
 140 threshold curvatures for cyclonic and anticyclonic rotations are $\pm 3.3 \times 10^{-6} \text{ m}^{-1}$, respectively,
 141 which are equivalent to a curvature radius of $\sim 3,000 \text{ km}$. It aims to practically remove the effect
 142 of planetary-scale waves, which are regarded as part of a background flow for transient eddies.
 143 Nevertheless, we have confirmed that results are qualitatively similar when a zero curvature
 144 threshold is used (Supplementary Fig. S2) or the effect of background planetary-scale waves is
 145 eliminated by spectral truncation (subtracting T4 winds from the total winds while calculating
 146 curvature) (Supplementary Fig. S3).

147 2.3 Energetics

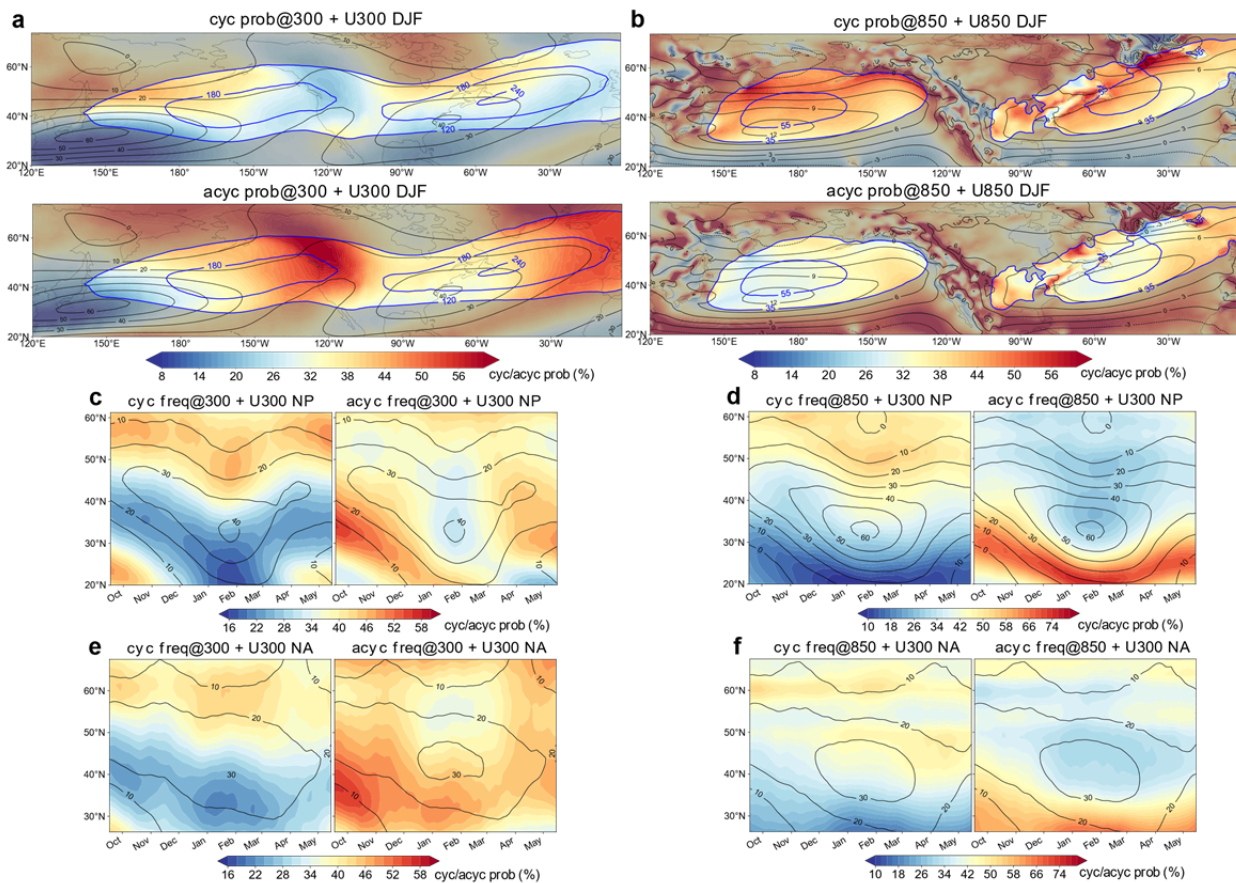
148 The formulation of energetics associated with transient eddy activity follows ONK22. To
 149 assess the relative importance of relevant processes independent of eddy amplitude, energy
 150 conversion/generation rates are normalized by the total eddy energy as the sum of EKE and
 151 EAPE (eddy available potential energy), which is not separated into cyclonic and anticyclonic
 152 contributions. The normalized rates are referred to as “*efficiencies*” (Kosaka & Nakamura, 2010;
 153 ONK22). The zonally-asymmetric climatological-mean state is considered as a background state
 154 for high-pass-filtered fluctuations. All the terms related to eddy energy and energy
 155 conversion/generation rates are three-dimensionally integrated over the NP [130°E–130°W,
 156 20°–65°N] or NA [80°–10°W, 25°–65°N] domain and from the surface to the 100-hPa level. In
 157 this study, energy conversion rates from low-frequency variability to sub-weekly eddies are
 158 neglected, because they are only of secondary importance (ONK22).

159

160 **3 Results**

161 3.1 Probability of cyclonic and anticyclonic regions

162 In the wintertime (DJF-mean) upper troposphere (Fig. 2a), cyclonic regions are more
 163 frequently observed north of the jet core region over each of the ocean basins. By contrast,
 164 anticyclonic regions are more frequent downstream of a jet core region. Note that those cyclonic
 165 and anticyclonic regions are identified through local curvature free from shear vorticity of a
 166 jetstream. The spatially contrasting probability of cyclonic and anticyclonic regions is common
 167 to the two major storm-tracks. In the lower troposphere (Fig. 2b), cyclonic regions are more
 168 frequent along a low-level eddy-driven jet axis as well as to its north, consistent with results
 169 based on cyclone tracking (Hoskins & Hodges, 2002; Shaw et al., 2016; ONK23).



170

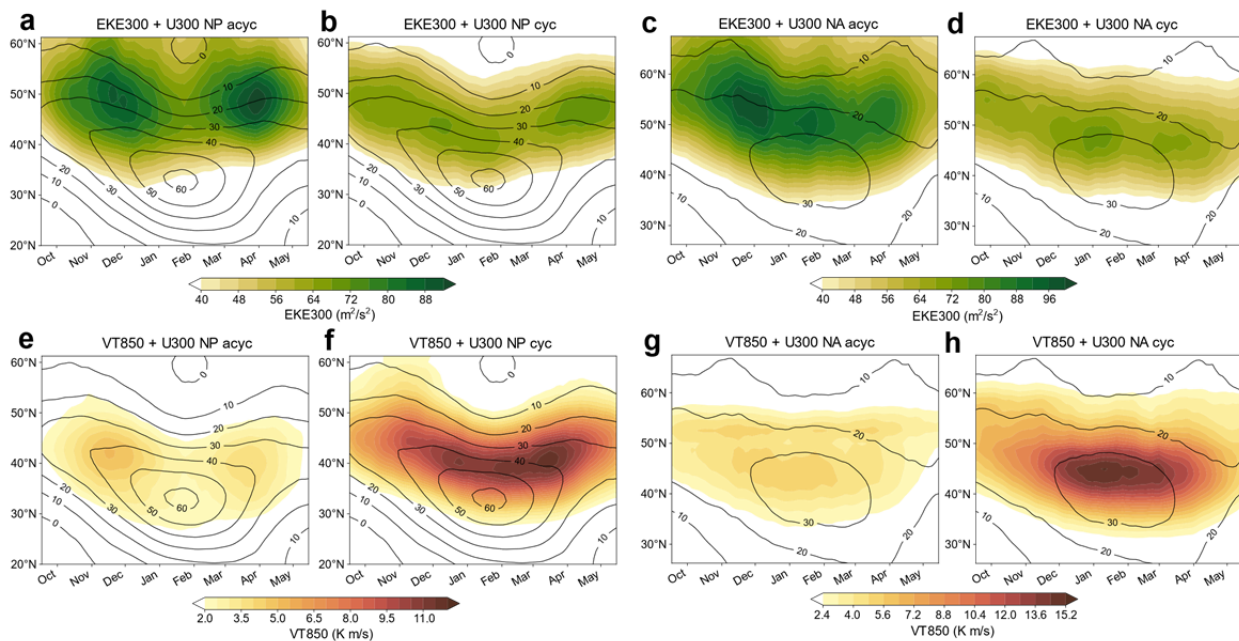
171 **Figure 2. Climatological-mean probability of cyclonic/anticyclonic regions and its**
 172 **seasonality. a-b** Climatological-mean wintertime (DJF) distributions of probability of cyclonic
 173 (upper) and anticyclonic (lower) regions (color, %) at 300-hPa (a) and 850-hPa (b). Black
 174 contours denote climatological-mean U_{300} (a) and U_{850} (b) (m/s). Blue contours signify
 175 climatological-mean EKE at 300 hPa (a) and 850 hPa (b) (m^2/s^2). **c** Climatological seasonality in
 176 probability of cyclonic (left) and anticyclonic (right) regions (color, %) at 300-hPa averaged for
 177 180°–150°W. Contours denote the corresponding seasonality of U_{300} averaged for 180°–150°W.
 178 **d** Same as in c, but for probability of cyclonic and anticyclonic regions at 850-hPa and U_{300}

179 averaged for $150^{\circ}\text{E}–180^{\circ}$. **e-f** Same as in c-d, respectively, but for probability of regions and
 180 U_{300} averaged for $70^{\circ}–40^{\circ}\text{W}$ (e) and $60^{\circ}–30^{\circ}\text{W}$ (f).

181 The climatological seasonality of the probability of lower-tropospheric cyclonic and
 182 anticyclonic regions (Fig. 2d) is consistent with the results based on tracking of NP surface
 183 migratory cyclones and anticyclones, respectively (ONK23). Over the midwinter NP, the
 184 probability of lower-tropospheric cyclonic region peaks, and its maximum expands equatorward
 185 under the strongest, equatorward-shifted Pacific jet. Contrastingly, the anticyclonic counterpart
 186 minimizes in midwinter around the storm-track axis near 40°N . The corresponding probability of
 187 upper-tropospheric cyclonic curvature exhibits a similar midwinter maximum and equatorward
 188 expansion (Fig. 2c). In comparison, over the NA, lower- and upper-tropospheric cyclonic regions
 189 exhibit less obvious seasonality than over the NP, as the NA jet exhibits only modest
 190 equatorward displacement and strengthening in midwinter (Figs. 2e-f).

191 3.2 Cyclonic and anticyclonic contributions to transient eddy activity

192 Figures 3a-d show the climatological seasonality of cyclonic and anticyclonic
 193 contributions to upper-tropospheric transient eddy activity over the NP and NA, where the latter
 194 contribution is overall greater than the former. The anticyclonic contribution to EKE_{300} exhibits a
 195 pronounced MWM under the strong NP jet (Fig. 3a), while the cyclonic counterpart does not
 196 minimize in midwinter (Fig. 3b). The distinct seasonality suggests that the anticyclonic
 197 contribution is predominantly responsible for the MWM of the total EKE_{300} (Fig. 1b). In contrast
 198 to the NP, the anticyclonic contribution to EKE_{300} over the NA does not exhibit a clear MWM
 199 (Fig. 3c). The cyclonic counterpart maximizes in midwinter (Fig. 3d). Their contributions
 200 correspond to the single peak in EKE_{300} over the NA (Fig. 1c).



201

202 **Figure 3. Seasonality of anticyclonic and cyclonic contributions to transient eddy activity.**
 203 **a-b** Climatological seasonality in EKE_{300} reconstructed only with anticyclonic (a) and cyclonic

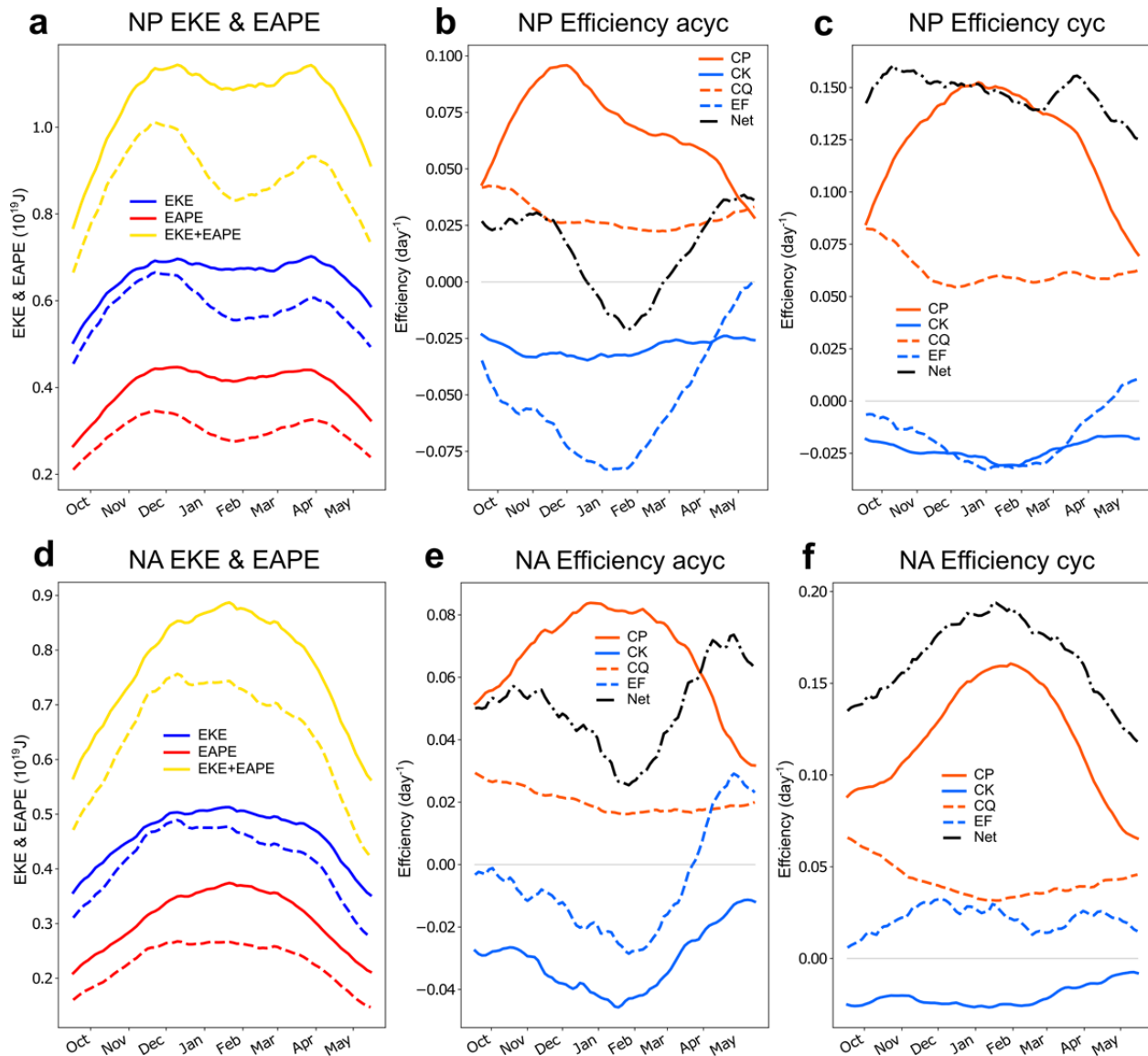
204 (b) regions averaged for 180° – 150° W. Contours denote the corresponding seasonality of
 205 climatological-mean U_{300} averaged for 150° E– 180° . **c-d** Same as in a-b, respectively, but for
 206 EKE_{300} averaged for 60° – 30° W. Contours denote the corresponding seasonality of
 207 climatological-mean U_{300} averaged for 70° – 40° W. **e-h** Same as in a-d, respectively, but for
 208 $V'T'_{850}$ averaged for 150° E– 180° (e-f) and 70° – 40° W (g-h).

209 The climatological seasonality of cyclonic and anticyclonic contributions to $V'T'_{850}$ also
 210 exhibits discernible differences between the NP and NA (Figs. 3e-h), similar to those of EKE_{300} .
 211 Although the anticyclonic contribution to $V'T'_{850}$ is overall substantially weaker (<50%) than the
 212 cyclonic counterpart as shown by ONK21, only the former exhibits an obvious MWM over the
 213 NP as the total $V'T'_{850}$ does (Figs. 3e and 1e). By contrast, the cyclonic contribution to $V'T'_{850}$ is
 214 rather constant throughout the winter with a slight peak in late winter (Fig. 3f). This is
 215 compatible with the midwinter peak in precipitation over the NP associated with cyclonic
 216 regions (Supplementary Figs. S4). Contrastingly, over the NA, both the cyclonic and
 217 anticyclonic contributions to $V'T'_{850}$ exhibit no clear MWM (Figs. 3f and 3h), contributing to the
 218 single midwinter peak in the total $V'T'_{850}$ (Fig. 1f).

219 3.3 Energetics

220 Quantitative evaluation of eddy energetics separately for the cyclonic and anticyclonic
 221 contributions delineates relevant processes for their distinct seasonality. We evaluate the
 222 “efficiency” of a given energetic term, whose reciprocal represents the time to replenish the
 223 three-dimensionally integrated total eddy energy ($EKE_{3D}+EAPE_{3D}$) over each of the entire NP
 224 and NA storm-track regions solely by that term, which is independent of the eddy amplitude
 225 (ONK22).

226 Over the NP (Fig. 4a), a more distinct MWM is observed for the anticyclonic
 227 contribution than for the cyclonic counterpart to each of EKE_{3D} , $EAPE_{3D}$, and $EKE_{3D}+EAPE_{3D}$,
 228 which is consistent with the preceding results (Fig. 3). Over the NA (Fig. 4d), contrastingly,
 229 those three types of eddy energy all peak in early- or mid-winter, regardless of the cyclonic or
 230 anticyclonic contribution. For both the NP and NA, the systematically larger cyclonic $EAPE_{3D}$
 231 compared to its anticyclonic counterpart may be an indication of the more baroclinic nature of
 232 migratory cyclones.



233

234 **Figure 4. Seasonality in the energetics regarding the anticyclonic and cyclonic**
 235 **contributions.** **a** Climatological-mean seasonal evolution of EKE_{3D} (blue), $EAPE_{3D}$ (red), and
 236 $EKE_{3D}+EAPE_{3D}$ (yellow) ($10^{19}J$). All the quantities plotted are integrated three-dimensionally
 237 over the NP. Solid and dashed lines signify the cyclonic and anticyclonic contributions,
 238 respectively. **b-c** Same as in a, but for “efficiency” (day^{-1}) of barotropic energy conversion (CK;
 239 blue), baroclinic energy conversion (CP; red), energy generation through diabatic processes (CQ;
 240 dashed red), and horizontal energy flux term (EF; dashed blue) contributed to by anticyclonic (b)
 241 and cyclonic regions (c) over the NP. Black dash-dotted lines denote the net efficiency relevant
 242 to the budget of $EKE_{3D}+EAPE_{3D}$ (viz. $CK+CP+CQ+EF$). **d-f** Same as in a-c, respectively, but for
 243 the NA.

244 The net “efficiency” of the energy conversion/generation terms associated with
 245 anticyclonic regions exhibits a distinct MWM over the NP (Fig. 4b). This is contributed to
 246 mainly by the declining positive efficiency of the baroclinic energy conversion (CP) from early
 247 winter and the reducing negative efficiency of the net energy flux term (EF) into spring. This

248 seasonality of the anticyclonic EF term is mainly due to the energy outflux through the eastern
249 boundary and the energy influx through the western boundary (Supplementary Fig. S5a), the
250 latter of which corresponds to the seeding effect from upstream (Penny et al., 2010). By contrast,
251 the net efficiency associated with cyclonic regions over the NP exhibits only a slight minimum in
252 early March (Fig. 4c), while systematically higher than its anticyclonic counterpart throughout
253 the cold season. Among the cyclonic contributions evaluated, the CP term exhibits the highest
254 efficiency with the most pronounced peak in midwinter.

255 The anticyclonic contribution to the net efficiency of energy conversion/generation
256 exhibits a well-defined MWM also over the NA (Fig. 4e). This is primarily due to the barotropic
257 energy conversion (CK) and EF terms, whose negative contribution maximizes in midwinter,
258 acting against the midwinter maximum of the CP efficiency. In midwinter, the energy outflux
259 maximizes, while the energy influx from the upstream minimizes (Supplementary Fig. S5b). In
260 comparison, the net efficiency associated with cyclonic regions exhibits a sharp midwinter
261 maximum over the NA (Fig. 4f), due primarily to the pronounced midwinter maximum in the CP
262 efficiency. Unlike its anticyclonic counterpart, the cyclonic EF term is positive and does not
263 minimize in midwinter (Fig. 4f). In essence, both the less distinct MWM of the anticyclonic net
264 efficiency, and the more prominent midwinter maximum of the cyclonic counterpart, correspond
265 to the midwinter peak in the NA eddy activity (Figs. 1e-f).

266 For both the NP and NA, the efficiency of the total diabatic energy generation (CQ) is
267 positive throughout the cold season with a slight MWM over the NA (Figs. 4b-c and 4e-f). This
268 is due to a midwinter offset between the maximized generation through precipitation and
269 maximized damping through air-sea heat exchange represented as the vertical diffusion term
270 (Supplementary Figs. S5c-d). This offset is more evident in the cyclonic contribution.

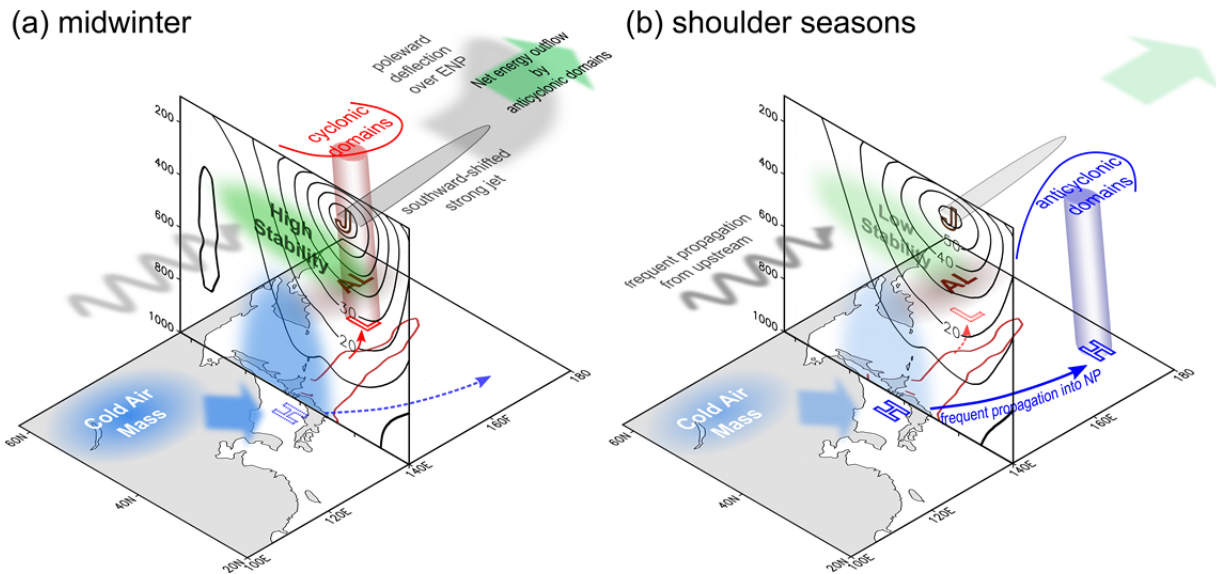
271

272 **4 Conclusions**

273 Utilizing a novel method for separate identification of cyclonic and anticyclonic regions
274 with local flow curvature (ONK21), this study demonstrates that the anticyclonic contribution to
275 transient eddy activity plays a pivotal role in setting its MWM over the NP. We thus posit that
276 not only cyclones but also anticyclones need to be considered in investigating transient eddy
277 activity measured as Eulerian eddy statistics, which has been ignored in previous studies. The
278 importance of anticyclones is compatible with the fact that the MWM of the NP transient eddy
279 activity has been reproduced in Eulerian statistics even in coarse-resolution GCMs (Christoph et
280 al., 1997; Zhang & Held, 1999).

281 For the contrasting seasonality of cyclonic and anticyclonic contributions to transient
282 eddy activity, their probability is also found important (Fig. 2). We, therefore, hypothesize that
283 the MWM of surface migratory anticyclone density over the NP (ONK23) is one of the crucial
284 factors for the MWM of transient eddy activity. Figure 5 schematically depicts factors giving rise
285 to the MWM of transient eddy activity over the NP, based on the results in this study in
286 combination with the distinct seasonality of NP surface migratory cyclones and anticyclones
287 (ONK23). An important factor, which is unique to the NP storm-track, is midwinter suppression
288 of the genesis of migratory surface anticyclones around the Japan Sea under the intensified

289 monsoonal northwesterlies and southward-shifted upper-level jet (ONK23). Another factor is the
 290 midwinter maximum of the eddy energy outflux from the eastern NP associated mainly with
 291 anticyclonic regions. The tendency of migratory anticyclones to propagate farther downstream
 292 compared to cyclones that exhibit a poleward-propagating tendency away from the jet because of
 293 diabatic heating (Tamarin & Kaspi, 2016; Tamarin & Kaspi, 2017) may also be relevant.



294

295 **Figure 5. Schematic of seasonality of the North Pacific transient eddy activity.**

296 Climatological-mean situations in (a) midwinter and (b) shoulder seasons. Black contours on
 297 vertical sections indicate climatological-mean westerly wind speed (m/s) averaged for
 298 130°–140°E in (a) midwinter (around 24Jan) and (b) early spring (around 19Mar).

299 The seasonality of the net efficiency is still asymmetric between the cyclonic and
 300 anticyclonic contributions even after normalized by their probability over the NP and NA
 301 (Supplementary Fig. S6). This suggests that intrinsic cyclone-anticyclone asymmetry may exist
 302 regardless of their probability. An intriguing finding is that the net efficiency only of the
 303 anticyclonic energy conversion/generation terms exhibits a distinct MWM both over the NP and
 304 NA. Potentially relevant factors regarding the asymmetry include diabatic heating, gradient wind
 305 balance, and typical moving direction, which will be covered by our future studies.

306 How the contrasting cyclonic and anticyclonic contributions lead to the MWM as their
 307 net effect is yet to be understood. Applying the framework used in this study to idealized GCM
 308 experiments with zonally-symmetric configurations (as by Novak et al., 2020; Yuval et al., 2018)
 309 will be informative. The MWM of the NA transient eddy activity under the extremely strong jet
 310 years (Afargan & Kaspi, 2017; Montoya Duque et al., 2021) may also be relevant for
 311 understanding the mechanism.

312 Finally, this study suggests that we should consider an anticyclonic contribution in
 313 investigating transient eddy activity in the warmed future climate (Eyring et al., 2021;
 314 Seneviratne et al., 2021), in which the westerly jet is overall projected to shift or expand
 315 poleward. Such investigations have been carried out either by Eulerian eddy statistics (Harvey et

316 al., 2020) or by cyclone tracking (Priestley & Catto, 2022). The “hybrid” perspective would be
317 helpful for a deeper understanding of future changes in storm-track activity.

318

319 **Acknowledgments**

320 This study is supported in part by the Japanese Ministry of Education, Culture, Sports, Science
321 and Technology (MEXT) through the Arctic Challenge for Sustainability II (ArCS-II;
322 JPMXD1420318865) and through the advanced studies of climate change projection (SENTAN;
323 JPMXD0722680395, by the Japan Science and Technology Agency through COI-NEXT
324 JPMJPF2013, by the Japanese Ministry of Environment through Environment Research and
325 Technology Development Fund JPMEERF20222002, and by the Japan Society for the
326 Promotion of Science (JSPS) through Grants-in-Aid for Scientific Research 19H05702 (on
327 Innovative Areas 6102), 20H01970, 22H01292, and 22K14097. Y.K. acknowledges support
328 from the JSPS Invitational Fellowship for Research in Japan that supported a sabbatical at the
329 University of Tokyo and ignited this collaboration, for support from the Research Center for
330 Advanced Technology and Science at the University of Tokyo and the Israeli Science
331 Foundation (grant 996/20).

332

333 **Open Research**

334 The JRA-55 reanalysis is available online at https://jra.kishou.go.jp/JRA-55/index_en.html. The
335 GPCP v3.2 monthly precipitation data is available online at
336 https://disc.gsfc.nasa.gov/datasets/GPCPMON_3.2/summary?keywords=GPCPMON. Inkscape
337 v1.0.1 (<https://inkscape.org/>) is used to generate the figures.

338

339 **References**

340 Afargan, H., & Kaspi, Y. (2017). A midwinter minimum in North Atlantic storm track intensity
341 in years of a strong jet. *Geophysical Research Letters*, 44(24), 12–511

342 Blackmon, M. L. (1976). A climatological spectral study of the 500 mb geopotential height of
343 the Northern Hemisphere. *Journal of the Atmospheric Sciences*, 33(8), 1607–1623.

344 Blackmon, M. L., Wallace, J. M., Lau, N.-C., & Mullen, S. L. (1977). An Observational Study of
345 the Northern Hemisphere Wintertime Circulation. *Journal of the Atmospheric Sciences*, 34(7),
346 1040–1053.

347 Chang, E. K. M. (2001). GCM and Observational Diagnoses of the Seasonal and Interannual
348 Variations of the Pacific Storm Track during the Cool Season. *Journal of the Atmospheric*
349 *Sciences*, 58(13), 1784–1800.

350 Chang, E. K. M., Lee, S., & Swanson, K. L. (2002). Storm track dynamics. *Journal of Climate*,
351 15(16), 2163–2183.

352 Christoph, M., Ulbrich, U., & Speth, P. (1997). Midwinter suppression of North Hemisphere
353 storm track activity in the real atmosphere and in GCM experiments. *Journal of the Atmospheric*
354 *Sciences*, 54(12), 1589–1599.

355 Deng, Y., & Mak, M. (2005). An Idealized Model Study Relevant to the Dynamics of the
356 Midwinter Minimum of the Pacific Storm Track. *Journal of the Atmospheric Sciences*, 62(4),
357 1209–1225.

358 Eady, E. T. (1949). Long Waves and Cyclone Waves. *Tellus*, 1(3), 33–52.

359 Eyring, V., Gillett, N. P., Achutarao, K., Barimalala, R., Barreiro Parrillo, M., Bellouin, N., et al.
360 (2021). Human Influence on the Climate System. *Climate Change 2021: The Physical Science*
361 *Basis. Contribution of Working Group I to the Sixth Assessment Report of the Intergovernmental*

- 362 *Panel on Climate Change*. V. Masson-Delmotte, P. Zhai, A. Pirani, S. L. Connors, C. Péan, S.
363 Berger, et al., Eds. Pp. 423–552, Cambridge Univ. Press.
- 364 Hadas, O., & Kaspi, Y. (2021). Suppression of Baroclinic Eddies by Strong Jets. *Journal of the*
365 *Atmospheric Sciences*, 78(8), 2445–2457.
- 366 Harada, Y., Kamahori, H., Kobayashi, C., Endo, H., Kobayashi, S., Ota, Y., et al. (2016). The
367 JRA-55 Reanalysis: Representation of Atmospheric Circulation and Climate Variability. *Journal*
368 *of the Meteorological Society of Japan*, 94(3), 269–302.
- 369 Harvey, B. J., Cook, P., Shaffrey, L. C., & Schiemann, R. (2020). The response of the northern
370 hemisphere storm tracks and jet streams to climate change in the CMIP3, CMIP5, and CMIP6
371 climate models. *Journal of Geophysical Research*, 125(23), e2020JD032701.
- 372 Hoskins, B. J., & Hodges, K. I. (2002). New Perspectives on the Northern Hemisphere Winter
373 Storm Tracks. *Journal of the Atmospheric Sciences*, 59(6), 1041–1061.
- 374 Hotta, D., & Nakamura, H. (2011). On the Significance of the Sensible Heat Supply from the
375 Ocean in the Maintenance of the Mean Baroclinicity along Storm Tracks. *Journal of Climate*,
376 24(13), 3377–3401.
- 377 Hurrell, J. W. (1995). Transient Eddy Forcing of the Rotational Flow during Northern Winter.
378 *Journal of the Atmospheric Sciences*, 52(12), 2286–2301.
- 379 James, I. N. (1987). Suppression of baroclinic instability in horizontally sheared flows. *Journal*
380 *of the Atmospheric Sciences*, 44(24), 3710–3720.
- 381 Kaspi, Y., & Schneider, T. (2011). Winter cold of eastern continental boundaries induced by
382 warm ocean waters. *Nature*, 471(7340), 621–624.
- 383 Kaspi, Y., & Schneider, T. (2013). The Role of Stationary Eddies in Shaping Midlatitude Storm
384 Tracks. *Journal of the Atmospheric Sciences*, 70(8), 2596–2613.

- 385 Kobayashi, S., Ota, Y., Harada, Y., Ebita, A., Moriya, M., Onoda, H., et al. (2015). The JRA-55
386 Reanalysis: General Specifications and Basic Characteristics. *Journal of the Meteorological*
387 *Society of Japan*, 93(1), 5–48.
- 388 Kosaka, Y., & Nakamura, H. (2010). Mechanisms of Meridional Teleconnection Observed
389 between a Summer Monsoon System and a Subtropical Anticyclone. Part I: The Pacific–Japan
390 Pattern. *Journal of Climate*, 23(19), 5085–5108.
- 391 Lee, S., & Kim, H.-K. (2003). The Dynamical Relationship between Subtropical and Eddy-
392 Driven Jets. *Journal of the Atmospheric Sciences*, 60(12), 1490–1503.
- 393 Montoya Duque, E., Lunkeit, F., & Blender, R. (2021). North Atlantic midwinter storm track
394 suppression and the European weather response in ERA5 reanalysis. *Theoretical and Applied*
395 *Climatology*, 144(3), 839–845.
- 396 Nakamura, H. (1992). Midwinter Suppression of Baroclinic Wave Activity in the Pacific.
397 *Journal of the Atmospheric Sciences*, 49(17), 1629–1642.
- 398 Nakamura, H., & Sampe, T. (2002). Trapping of synoptic-scale disturbances into the North-
399 Pacific subtropical jet core in midwinter. *Geophysical Research Letters*, 29(16), 1–4.
- 400 Nakamura, H., Sampe, T., Tanimoto, Y., & Shimpo, A. (2004). Observed associations among
401 storm tracks, jet streams and midlatitude oceanic fronts. *Earth’s Climate: The Ocean–*
402 *Atmosphere Interaction*, *Geophys. Monogr*, 147, 329–345.
- 403 Novak, L., Schneider, T., & Ait-Chaalal, F. (2020). Midwinter Suppression of Storm Tracks in
404 an Idealized Zonally Symmetric Setting. *Journal of the Atmospheric Sciences*, 77(1), 297–313.
- 405 Okajima, S., Nakamura, H., & Kaspi, Y. (2021). Cyclonic and anticyclonic contributions to
406 atmospheric energetics. *Scientific Reports*, 11(1), 13202.

- 407 Okajima, S., Nakamura, H., & Kaspi, Y. (2022). Energetics of transient eddies related to the
408 midwinter minimum of the North Pacific storm-track activity. *Journal of Climate*, 35(4), 1137–
409 1156.
- 410 Okajima, S., Nakamura, H., & Kaspi, Y. (2023). Distinct roles of cyclones and anticyclones in
411 setting the midwinter minimum of the North Pacific eddy activity: a Lagrangian perspective.
412 *Journal of Climate*, 36(14), 4793–4814.
- 413 Penny, S., Roe, G. H., & Battisti, D. S. (2010). The Source of the Midwinter Suppression in
414 Storminess over the North Pacific. *Journal of Climate*, 23(3), 634–648.
- 415 Priestley, M. D. K., & Catto, J. L. (2022). Future changes in the extratropical storm tracks and
416 cyclone intensity, wind speed, and structure. *Weather and Climate Dynamics*, 3(1), 337–360.
- 417 Schemm, S., & Rivière, G. (2019). On the Efficiency of Baroclinic Eddy Growth and How It
418 Reduces the North Pacific Storm-Track Intensity in Midwinter. *Journal of Climate*, 32(23),
419 8373–8398.
- 420 Seneviratne, S. I., Zhang, X., Adnan, M., Badi, W., Dereczynski, C., Di Luca, A., et al. (2021).
421 Weather and climate extreme events in a changing climate. *Climate change 2021: The physical*
422 *science basis. Contribution of working group I to the sixth assessment report of the*
423 *intergovernmental panel on climate change* (pp. 1513–1766). V. Masson-Delmotte, P. Zhai, A.
424 Pirani, S. L. Connors, C. Péan, S. Berger, et al. (Eds.), Cambridge University Press.
- 425 Shaw, T. A., Baldwin, M., Barnes, E. A., Caballero, R., Garfinkel, C. I., Hwang, Y.-T., et al.
426 (2016). Storm track processes and the opposing influences of climate change. *Nature*
427 *Geoscience*, 9(9), 656–664.
- 428 Tamarin, T., & Kaspi, Y. (2016). The Poleward Motion of Extratropical Cyclones from a
429 Potential Vorticity Tendency Analysis. *Journal of the Atmospheric Sciences*, 73(4), 1687–1707.

- 430 Tamarin, T., & Kaspi, Y. (2017). The poleward shift of storm tracks under global warming: A
431 Lagrangian perspective. *Geophysical Research Letters*, 44(20), 10666–10674.
- 432 Wallace, J. M., Lim, G.-H., & Blackmon, M. L. (1988). Relationship between Cyclone Tracks,
433 Anticyclone Tracks and Baroclinic Waveguides. *Journal of the Atmospheric Sciences*, 45(3),
434 439–462.
- 435 Yuval, J., Afargan, H., & Kaspi, Y. (2018). The relation between the seasonal changes in jet
436 characteristics and the pacific midwinter minimum in eddy activity. *Geophysical Research*
437 *Letters*, 45(18), 9995–10002.
- 438 Zhang, Y., & Held, I. M. (1999). A linear stochastic model of a GCM's midlatitude storm tracks.
439 *Journal of the Atmospheric Sciences*, 56(19), 3416–3435.